

# Coated fused silica fibers for enhanced sensitivity torsion pendulum

Kenji Numata<sup>a,b,1</sup>, Jordan Horowitz<sup>c</sup>, and Jordan Camp<sup>b</sup>

<sup>a</sup> *Department of Astronomy, University of Maryland, College Park, Maryland, 20742, USA*

<sup>b</sup> *NASA Goddard Space Flight Center, Code 663, 8800 Greenbelt Rd., Greenbelt, Maryland, 20771, USA*

<sup>c</sup> *Department of Physics, University of Maryland, College Park, Maryland, 20742, USA*

---

## Abstract

In order to investigate the fundamental thermal noise limit of a torsion pendulum using a fused silica fiber, we systematically measured and modeled the mechanical losses of thin fused silica fibers coated by electrically conductive thin metal films. Our results indicate that it is possible to achieve a thermal noise limit for coated silica lower by a factor between 3 and 9, depending on the silica diameter, compared to the best tungsten fibers available. This will allow a corresponding increase in sensitivity of torsion pendula used for weak force measurements, including the gravitational constant measurement and ground-based force noise testing for the LISA mission.

*PACS:* 05.40.Jc; 07.10.Pz; 06.30.Bp; 04.80.Nn; 07.87.+v

*Keywords:* Fused silica; Torsion pendulum; Quality factor; Thermal noise; Thin film; Gravitational wave detectors

---

---

<sup>1</sup> Corresponding author: numata@milkyway.gsfc.nasa.gov.

## 1 Introduction

The torsion pendulum has been widely used for measuring weak forces on the ground, such as gravity. The torsion pendulum is composed of a mass supported by a thin fiber with a very low rotational resonant frequency. Thus the mass acts nearly as a free mass for the rotational degree of freedom and is highly sensitive to external forces. Measurement applications include fundamental physics tests such as equivalence principle test [1] and the gravitational constant measurement [2], as well as practical tests, such as force noise measurement of low-frequency accelerometers. In particular, the accelerometer used in the Laser Interferometer Space Antenna (LISA) [3] is designed to have one of the smallest force noise ever measured and is studied with a torsion pendulum [4].

The fundamental noise limitation in the operation of the torsion pendulum is thermal noise (fluctuation) associated with the mechanical loss (dissipation) in suspending fibers. According to the Fluctuation-Dissipation Theorem (FDT) [5], the amplitude of thermal noise is proportional to the mechanical loss of the fiber [6]. Tungsten has been used as the fiber material for the highest sensitivity measurements to date because it can be easily handled, it has relatively small mechanical loss for a metal and it has high breaking strength.

Fused silica is known to have very small mechanical losses compared to metal and other kinds of amorphous glasses. Consequently, it is used in ultra sensitive measurements where thermal noise plays an important role. Ground-based interferometric gravitational wave detectors [7] adopt fused silica as mirror substrates and suspension fibers for this reason. In this field, mechanical loss of fused silica has been intensively measured in the kilohertz range [8]. The measured smallest loss angle,  $\phi$ , which is the measure of mechanical loss, reached  $2 \times 10^{-9}$  level [9]. This level is substantially smaller than that of tungsten fibers — typically  $5 \times 10^{-4}$  [1, 4] in  $10\mu\text{m}$  diameter region. Therefore, fused silica has the potential to lower the thermal noise limit in force noise measurements, when used as a suspension fiber instead of commonly-used tungsten. However, in order to avoid electrostatic stray forces the pendulum and the fiber must be set at fixed electrical potential. The additional step of coating a fused silica fiber with a conductor must be taken, since fused silica is an insulator.

In this paper, we show fused silica fiber coated with a conducting thin metal film can have small mechanical loss. The thickness of the metal coating must be thin, so that the mechanical loss induced by the coating metal is minimized. Bismuth (Bi) was selected as a main top layer coating material through mechanical loss measurements. We also used germanium (Ge) as a sub layer under the Bi to provide a highly adherent surface that kept a very thin Bi layer

continuous and conductive. We built a system to pull thin fused silica fibers, a coater to uniformly coat the fibers with two different materials and a Q-measurement apparatus to measure the loss of the fiber in torsion pendulum. Our results indicate that it is possible to make conductive fused silica fibers with a lower fundamental thermal noise limit by a factor of 3 to 9, depending on the silica fiber diameter, compared to the highest Q tungsten fibers. This will allow higher precision study of fundamental gravitational measurements and could make ground based force noise testing a factor 35 closer to the LISA requirements.

## 2 Experimental method

In this section, we first describe our silica fibers pulled from silica rods. Then we explain our evaporator to coat fibers. Finally, we introduce the torsion pendulum setup to measure the mechanical loss of fibers.

### 2.1 *Silica fibers*

The silica fibers were pulled from Heraeus [10] Suprasil-2 rods with diameters of 1mm, 2mm, 3mm, and 4mm, using oxygen-hydrogen flame. Suprasil-2 is known to have small mechanical loss at kilohertz frequency range [8]. Figure 1 shows the fiber pulling machine. The rods were hung vertically with the center heated and melted by the flame. As the bottom end of the rod falls due to gravity and passes in front of a reflective sensor, it turns off the flame, with a resultant thin fiber length of about 250mm. On both ends of the fiber were two end tabs  $\sim 1.5$  cm long having the diameter of the rod. The thickness variation over the thin fiber was about 20%. The diameter of the final thin fiber ranged from  $10\mu\text{m}$  to  $110\mu\text{m}$  depending on the original rod diameter and size of the flame.

### 2.2 *Evaporator to coat fibers*

After pulling, the fiber was carefully cleaned with alcohol and vertically hung in a vacuum tank for coating. We used a thermal evaporation technique to form thin film on the fiber surface. Figure 2 shows the inside of the evaporation vacuum tank. The tank has two evaporation boats made of tungsten. The temperature of the boats can be controlled independently from outside of the tank. To get uniform coating across the surface, the fiber was rotated at a speed of  $\sim 30\text{rpm}$ . In addition, a blocking mask was designed and placed

around the fiber to get uniform coating over the length. The mask was made out of cylindrical shell with a larger opening at the higher end of the cylinder, which compensated for the increased distance from the top to the evaporation boats. The mask was rotated around the fiber at a speed of  $\sim 10$ rpm. Using the rotating coating mask, the resultant coating thickness variation over the fiber length was kept smaller than  $\pm 10\%$ . Figure 3 shows the coating thickness distribution measured inside and outside of the mask, using glass plates as shown in Fig. 2. During the evaporation process, the coating thickness on fiber was determined from a readout of a quartz thickness monitor which was located at a height of the fiber middle but outside of the mask. The coating on the glass plates were used to calibrate the coating thickness on fiber. The vacuum level during evaporation was typically below  $10^{-5}$ Torr. After the fiber was taken out from the vacuum tank, the fiber resistance over the length was measured with a digital multimeter. We also performed coatings on standard microscope slides held outside of the mask in order to study the resistance dependence on coating thickness.

In order to minimize the mechanical loss induced by the metal coating, it is desirable to keep the thickness of the coating as thin as possible. At the same time, uniform and continuous coating is necessary from the viewpoint of electrical conductivity and shielding. Usually, very thin films ( $< 100\text{\AA}$ ) are discontinuous; many metals tend to form discrete islands due to high mobility of the evaporant flux on the substrate surface. A several monolayer thick film of Ge is known to form a highly adherent amorphous film and to inhibit the discrete structure of material deposited on top of the Ge film [11]. We used this technique to provide a conductive layer of minimal thickness. As a top layer material, we tested Bi, gold (Au), and aluminum (Al). We investigated Bi mainly because of its small mechanical loss (shown below).

### *2.3 Torsion pendulum to measure mechanical loss of fiber*

After pulling and coating, the fibers were installed into another vacuum tank for mechanical loss measurement. To do this we monitored the amplitude decay, or ringdown, of a torsion pendulum using the fiber. Figure 4 shows the conceptual setup. Two small cups made of aluminum were attached on the two thick ends of the fiber. One of the cups was fixed to a frame and a pendulum was attached on the other cup. The vacuum tank contained 5 pendula, whose weight ranged from 6g to 60g, and allowed us to perform 5 measurements at a time. The rotational motion of each pendulum was detected by a shadow sensor, which is composed of an infrared LED and a silicon photodiode. As the pendulum swung, some of the infrared light was blocked by the pendulum, causing a change in the photodiode output. The rotational resonant frequency of the pendulum ranged from 6mHz to 78mHz depending

on the thickness of fiber and the pendulum weight (inertia). The data was recorded by a computer and then processed with a software lock-in amplifier to see the decay envelope of the rotational motion. Then the envelope was fit to an exponential function,  $\exp(-\pi f_0 t / Q_{\text{pend}})$ , where  $f_0$  is resonant frequency,  $t$  is time, and  $Q_{\text{pend}}$  is quality factor, which is inverse of mechanical loss angle,  $\phi_{\text{pend}}$ . The pendulum loss  $\phi_{\text{pend}}$  is identical to the fiber loss  $\phi_{\text{fiber}}$  in the case of torsion pendula. Typical vacuum level during the ring down measurement was  $8 \times 10^{-8}$  Torr, which required a 100°C vacuum bakeout. The 1-m diameter, 1-m height vacuum system was pumped by a 500 l/s turbo pump, and its final pressure was probably limited by permeation through its O-rings. The typical measurement time of the pendulum ringdown was 3 days.

### 3 Experimental results and analysis

In this section, we show our experimental results showing our loss analysis model. We first selected a main coating material by directly measuring the loss of the material. Then we selected the thickness of the coating. Finally, we measured mechanical loss of the coated fibers in a torsion pendulum.

#### 3.1 Coating loss model and loss measurement of uncoated fiber

In order to determine the mechanical loss of each metal, we first measured the ringdown of uncoated fibers with different diameters. We then measured fibers coated with relatively thick metal coatings (over 200 Å) to enhance the additional loss caused by the coating.

The loss of the fiber is the sum of the loss of fused silica,  $\phi_{\text{SiO}_2}$ , and the loss due to the coating. In a torsion mode, strain energy due to the fiber rotation is distributed evenly over the cross section. Therefore, the effect of coating material loss,  $\phi_{\text{mat}}$ , on the fiber is diluted by a ratio of the cross sectional area ( $\pi dh$  to  $\pi d^2/4$ ), where  $h$  is the coating thickness,  $d$  is the fiber diameter, and  $d \gg h$ . Therefore, we get

$$\phi_{\text{fiber}} = \phi_{\text{SiO}_2} + \frac{4h}{d}\phi_{\text{mat}}. \quad (1)$$

Note that material loss  $\phi_{\text{mat}}$  is defined so that it is independent of geometry. In order to model the loss of fused silica  $\phi_{\text{SiO}_2}$ , we performed a set of measurements on uncoated fibers. Square markers in Fig. 5 show the measured loss dependence on fiber diameter. Figure 6-(A) shows an example of decay curve of an uncoated fiber.

To interpret our results we assumed the structural damping model [6], where the loss depends on the fiber diameter but does not depend on the resonant frequency. This interpretation is supported by the fact that we did not measure any obvious frequency dependence of loss. For simplicity, we also assumed structural damping model for the coating material. In addition, we neglected the difference in shear modulus between materials.

By fitting the measured loss data with uncoated fibers to the model proposed in [12], assuming that surface loss is the largest contributor in our range of fiber diameter, we derived

$$\phi_{\text{SiO}_2} = 5.9 \times 10^{-9} (1 + 1.7 \times 10^{-2} / d[\text{m}]) \quad (2)$$

as the modeled loss of our uncoated silica fibers. The dotted line in Fig. 5 shows this model. This is factor  $\sim 2$  larger than that of previously reported results [12, 13] in our diameter range. It might be due to differences in silica brand, surface condition, and frequency range. It might also be related to the smallness of the breaking strength of our fiber (shown below).

### *3.2 Selection of coating material by thick single layer coating*

The coating material losses  $\phi_{\text{mat}}$  were calculated from the measured coated fiber loss, Eq.(1), and the modeled silica fiber loss (Eq.(2)). The results are summarized in Table 1. Ge had the smallest loss among the materials we tested, presumably because of its inherent hardness. This suggested that Ge would be useful as an under layer adhesive to a conductive upper coating, while adding minimal loss. Bi, Al, and Au were the candidate conductive materials in this experiment, because of their low melting temperatures and ease in handling. Bi was easily evaporated and had the smallest loss. Au is commonly used as an evaporation material to make smooth conductive surfaces. Although its evaporation rate control was easy, it turned out that it has the largest mechanical loss. The large loss is probably related to the softness of the Au film. We found it difficult to make consistent thin films of Al. According to this result, Ge and Bi were selected to be the most promising combination to keep coating loss small. In this paper, we present the results with this combination of materials.

### *3.3 Selection of coating thickness by resistivity measurement*

In coating the silica fibers, our goal was to minimize the coating loss while at the same time ensuring that the coating was uniform and conductive. To

determine the necessary thickness of the Bi and Ge coatings, we measured resistivity of various thicknesses of Bi/Ge coating on silica fibers and easily available glass slides. In Fig. 7, resistivity is plotted against the thickness of Bi, for three different thickness of the Ge sublayer. Markers with connecting lines show the results with glass slides, while unconnected markers show results for coated fibers. The data shows that as the thickness of Bi becomes smaller, the resistivity stays roughly constant until a threshold is reached, where it increases rapidly. The threshold level for rapid resistivity increase is related to the thickness of the Ge sublayer. This is understood to be due to the onset of discontinuity of the Bi film [11], which is inhibited by the adhesive Ge sublayer. Thus the use of a Ge sublayer allows us to minimize the thickness of the more lossy Bi conductive coating.

To ensure continuous robust surface coating, we used Bi and Ge thickness in the constant resistivity region to coat the fibers. The physical effect of the Ge sublayer may be seen in the following photos. When evaporated as a thin film, Bi tends to grow in incoherent directions forming small crystal grains. Figure 8-(a) shows a photo of the surface of 50Å-Bi coated fiber taken by a scanning electron microscope. The structure seen in the photo indicates the non-uniform crystal growth. Figure 8-(b) shows the surface coated by 300Å-Bi. With this thickness, the coating becomes continuous. However, it is not smooth due to a large grain structure. Figure 8-(c) shows the surface coated by 100Å-Bi with 50Å-Ge under layer. The Ge sublayer is seen to smooth the non-uniform structure.

### 3.4 Resistivity and loss measurement of coated silica fibers

Conductive fibers were successfully obtained using the values within the constant resistivity region in Fig. 7. Typical resistance over the fiber length was  $1\text{M}\Omega$ . Unconnected markers shows the resistivity of the Bi coating on the fibers. They mostly showed lower resistivity than that obtained with glass slides. This is probably due to the surface quality and material differences of the glass slide and fiber. The data scatter may be due to variations in fiber surface condition. The fiber surface is believed to be very smooth, because it is effectively polished by the flame when the fiber is pulled. However, the process is difficult to control precisely, and microscopic structure of surface may vary fiber to fiber. The tapered fiber ends adds errors in the calculation of resistivity as well.

The mechanical loss of the coated conductive fibers was measured using the pendulum. Round markers in Fig. 5 show the measured loss dependence on fiber diameter. They showed larger loss than uncoated silica fibers as expected. Figure 6-(B) shows an example of decay curve of a coated fiber.

## 4 Discussion

In this section, we first discuss the application of our results to the improvement in sensitivity of small force measurements. Next we use our data to verify our mechanical loss model. Then we evaluate the loss due to residual gas and measurement errors. Finally, we present our ideas to further improve the performance of the coated fibers and applications to other fields.

### 4.1 Sensitivity gain factor in force noise measurement

According to the FDT, the thermal noise limit of force noise in torsion pendula is given by the following [4]:

$$S_{\text{TN}}^{1/2}(f) = \sqrt{\frac{4k_{\text{B}}T\kappa\phi_{\text{fiber}}}{2\pi f}}. \quad (3)$$

Here,  $\kappa = \pi d^4 G / (32L)$ ,  $k_{\text{B}}$  is the Boltzman constant,  $T$  is temperature,  $G$  is shear modulus of the fiber,  $L$  is the length of the fiber, and  $f$  is frequency.  $S_{\text{TN}}^{1/2}(f)$  is the spectrum density of the force (thermal) noise. In order to compare the noise level between tungsten and silica fibers, we evaluate  $\sqrt{d^4 G \phi_{\text{fiber}}}$  as a figure of merit. As a reference, we adopt  $d = 20(\mu\text{m})$  and  $\phi_{\text{fiber}} = 1/9000$  as the lowest mechanical loss tungsten fiber [14]. (This fiber was heat treated to lower its loss.) Shear modulus of silica is smaller than that of tungsten by a factor of 7. Then, if we take the measured silica values,  $d = 22(\mu\text{m})$  and  $\phi_{\text{fiber}} = 1/(9.5 \times 10^4)$  (indicated as (B) in Figs. 5 and 6), as an example, the figure of merit becomes 7.4 times smaller than that of tungsten. We refer to this as the gain factor of silica fiber. The gain factors were plotted against fiber diameters in Fig. 9. Since we fixed reference tungsten fiber diameter, the gain factor becomes larger with decreasing silica fiber diameter. The gain factor was about 3 for a  $\sim 40\mu\text{m}$  diameter fiber, and reached 9 for a  $11\mu\text{m}$  fiber (the thinnest we measured).

This result has a substantial impact on small force measurement. For example, in the test of the equivalence principle [1] and ground testing of LISA accelerometer called Gravitational Reference Sensor (GRS), the sensitivity is limited by thermal noise from suspension tungsten fibers. In the case of LISA GRS ground testing, using a tungsten fiber with  $25\mu\text{m}$  diameter and  $\phi_{\text{fiber}} = 1/1700$ , the sensitivity achieved was a factor 70 above the LISA requirement [4]. If our  $22\mu\text{m}$  conductive fiber was used in the same pendulum, the thermal noise limit should be pushed down to a factor 2 above the LISA requirement. Figure 10 shows the comparison of the noise level with tungsten and silica fibers together with LISA requirement. We assumed the same param-



eters except for the loss, diameter, and shear modulus. The non-fundamental sensor noise is limiting the sensitivity at higher frequency. At lower frequency, the thermal noise limit becomes much closer to the LISA requirement by the use of fused silica.

## 4.2 Breaking strength

In the design of torsion pendula, the breaking strength is an important consideration since it sets the weight limit of the suspended mass. Breaking strengths of tungsten and silica fibers are highly dependent on treatment. We found a typical breaking strength of our uncoated silica fiber of 0.5GPa, compared with breaking strength of typical tungsten fiber of 1GPa. However, there are several references that present significantly higher silica breaking strength [15]. Around 10 $\mu$ m diameter range, it appears possible to have  $\sim$ 10GPa breaking strength. Therefore, it should be possible to use same or smaller diameter silica fiber to support a mass, compared to the diameter necessary for a tungsten fiber. In this case the gain factor should become even larger. More research is necessary to establish the best silica fiber treatment to obtain the highest possible breaking strength. This should also help in improving the fragility of silica, which could make its installation easier.

## 4.3 Mechanical loss model

To explore our understanding of the loss mechanisms for the fully coated silica fiber, we analyzed our data in the following way. When we have two coating materials on a fiber in series, we can rewrite the mechanical loss model Eq.(1) as

$$\phi_{\text{fiber}} = \phi_{\text{SiO}_2} + \frac{4(h_1 + h_2)}{d} \phi_{\text{avg}}, \quad (4)$$

where

$$\phi_{\text{avg}} \equiv \frac{h_1 \phi_{\text{mat1}} + h_2 \phi_{\text{mat2}}}{h_1 + h_2}, \quad (5)$$

$h_i$  is the thickness and  $\phi_{\text{mat}i}$  is the loss of  $i$ -th material ( $i = 1, 2$ ).  $\phi_{\text{avg}}$  is the averaged loss over the two materials weighted by each thickness. We can calculate this loss value using the thickness of each coating and the independently measured loss listed in Table 1. We call this value expected averaged loss. We compared this with experimental loss results measured with fibers coated

with two materials, for all the fiber coating thicknesses shown in Fig. 7. Figure 11 shows the result. If our loss model is completely correct, the measured loss result (plotted as round markers) should fall onto the dotted line. The agreement appears reasonably good; except for the thinnest fiber data, every marker is within factor 3 from the expected line. However the measured data shows scatter around the expected line, which cannot be explained only by measurement errors. The reason of the discrepancy is possibly due to the imperfection of the silica loss model  $\phi_{\text{SiO}_2}$ , the inadequateness of the constant loss assumption over frequency and thickness and surface condition variations.

#### 4.4 Loss due to residual gas

The loss due to the residual gas is especially important when the pendulum resonant frequency is low and the loss to be measured is small. It is known that the residual gas loss is proportional to residual pressure,  $P$ , and the inverse of the resonant frequency,  $f_0$  [6]. We made a model of the residual gas loss acting on our pendulum,  $\phi_{\text{gas}}$ , by measuring the pendulum loss as a function of the vacuum level and by extrapolating it. The result was

$$\phi_{\text{gas}} = 1.2 \times 10^{-7} \frac{P}{10^{-7}[\text{Torr}]} \frac{10[\text{mHz}]}{f_0}. \quad (6)$$

At our vacuum system pressure of  $8 \times 10^{-8}$  Torr, the residual gas loss is small compared to the measured losses. Therefore, the loss due to residual gas is believed to have marginal effect on our loss measurements.

#### 4.5 Measurement errors

Error bars in Figs. 5, 7, 9, and 11 show measurement error estimates. Measurement error of fiber diameter was  $\pm 1\mu\text{m}$ . Coating thickness error was estimated to be  $\pm 10\%$ . These errors and uncertainty of tapered fiber ends are the cause of the resistivity error of 30% in Fig. 7. In this experiment, we assume measurement error in loss  $\phi$  to be  $\pm 30\%$ . This value was estimated by dividing the three day measurement into 1 day sub-intervals, and examining the consistency of the fitted decay times. This error in  $\phi$  is the biggest error source in Figs. 9 and 11. In order to evaluate this error more precisely, additional work is needed to reduce electrical and gravitational disturbances, which tended to affect decay curve data in lower frequency pendula.

#### 4.6 *Other possible technique*

There are a number of further possible techniques for producing conductive fibers with smaller loss. One promising possibility is to minimize the thickness of the total coating layer by using ion doping or implantation to lower the resistivity of the thin Ge layer, so that no additional thick metal coating is needed. To examine this possibility, we tested ion doping with indium (In) as a dopant on Ge. We coated polished glass with 100Å-Ge and 10Å-In and baked it at 500°C for 2 hours to thermally diffuse In into Ge. After baking the coating became successfully conductive. Although its resistivity was high ( $10^{-2}\Omega\text{m}$  level, which corresponds  $\sim 1\text{G}\Omega$  fiber resistance), we believe this direction is promising: if we assume a pendulum has a capacitance of 100pF,  $1\text{G}\Omega$  fiber will take  $\sim 0.1\text{s}$  for accumulated charge to dissipate, which is already small compared to the LISA timescale of 10 to  $10^4\text{sec}$ . In pursuing this direction there are many parameters to investigate, such as baking temperature, duration, dopant concentration and material. Gallium, copper, antimony and arsenic are the other possible dopants [16].

Once the loss due to coating is minimized by these techniques, the reduction of loss in silica itself will become more important. The silica loss might be improved by etching, annealing, and pulling with lasers possibly under vacuum. We estimate that another factor 2-3 in sensitivity gain should be possible with doped Ge and lowered silica loss.

Finally, the effect of coating on the fused silica breaking strength should be investigated. It is possible that the coating may raise the breaking strength by blocking water absorption into the silica surface micro cracks.

#### 4.7 *Application to other fields*

As far as the authors know, our work is the first systematic measurement of mechanical loss of silica fiber at low frequency using torsional mode. The continuing work will help understanding loss mechanism in bulk silica and its surface. The loss angle of thin metal film presented here is of interest for both our application to torsion pendulum fibers where mechanical damping is to be minimized, as well as for applications where damping is required [17]. Overall, this research will be of interest to ground-based gravitational wave group as well as other low-noise measurement groups.

## 5 Conclusion

We made fused silica fibers coated by thin metal films in order to minimize thermal noise and to enhance the sensitivity of torsion pendula for small force measurements. The diameters of our fibers were between  $10\mu\text{m}$  and  $110\mu\text{m}$ . We investigated Bi coating on a Ge adhesive under layer. Their typical thicknesses were  $100\text{\AA}$ . We successfully obtained electrical conductivity along the fiber with the thin coatings of order  $1\text{M}\Omega$ . The coating was believed to be smooth, continuous, and uniform. The mechanical loss measurement using torsion pendula shows that thermal noise of our coated fiber is smaller than that of lowest loss tungsten fiber by a gain factor of between 3 and 9. This implies that the ground testing of LISA GRS force noise with a torsion pendulum could reach to within a factor 2 of the LISA requirement. Although there are a several remaining issues to be investigated and tried, the use of coated silica fiber as torsion pendulum has proven to be a very promising approach to minimize the fundamental thermal noise limit.

## 6 Acknowledgements

We thank F. SanSebastian (NASA/GSFC) for his machining works and his continuous supports. We are grateful to Dr. L. Wang (NASA/GSFC) who helped us with his scanning electron microscope and with his knowledge about thin coating. We acknowledge A. Kemery (University of Maryland, Baltimore County) for her contribution in initial measurement environment setup. Finally, we thank Prof. David Tanner (University of Florida) for his consultation on the doping of Ge coatings. This research was supported in part by the 2003 Director's Discretionary Fund of NASA Goddard Space Flight Center and the Maryland Space Grant Consortium.

## References

- [1] G.L. Smith *et al.*, Phys. Rev. D 61 (1999) 022001.
- [2] J.H. Gundlach *et al.*, Phys. Rev. D 54 (1996) R1256.
- [3] K. Danzmann *et al.*, *LISA Pre-Phase A Report – Second Edition*, MPQ233, July (1998).
- [4] L. Carbone *et al.*, Phys. Rev. Lett. 91 (2003) 151101.
- [5] H.B. Callen and R.F. Greene, Phys. Rev. 86 (1952) 702.
- [6] P.R. Saulson, Phys. Rev. D 42 (1990) 2437.
- [7] *Gravitational Wave Detection*, edited by K. Tsubono, M.-K. Fujimoto, and K. Kuroda (University Academy Press, Tokyo, 1997).
- [8] K. Numata *et al.*, Phys. Lett. A 327 (2004) 263 and references therein.
- [9] A. Ageev *et al.*, Class. Quantum. Grav., 21 (2004) 3887.
- [10] Heraeus-Amersil Corporation, 3473 Satellite Boulevard, Duluth, GA 30136-5821.
- [11] J.B. Camp, T.W. Darling, and R.E. Brown, J. Appl. Phys., 71 (1992) 783.
- [12] A.M. Gretarsson and G.M. Harry, Rev. Sci. Instrum., 70 (1999) 4081.
- [13] I.A. Bilenko, V.B. Braginsky, and S.L. Lourié, Class. Quantum. Grav., 21 (2004) S1231.
- [14] Personal communication with J.H. Gundlach (Univ. of Washington).
- [15] A.M. Gretarsson, ArXiv:cond-mat/0205448.
- [16] Personal communication with D. Tanner (Univ. of Florida).
- [17] S. Goßler *et al.*, Class. Quantum. Grav., 21 (2004) S1231.

Material	Loss angle $\phi_{\text{mat}}$	Comment
Ge	$1.8 \times 10^{-3}$	Used as under layer. Non-conductive.
Bi	$5.8 \times 10^{-3}$	Easy to evaporate. Small loss.
Al	$8.0 \times 10^{-3}$	Difficult to control evaporation rate.
Au	$2.7 \times 10^{-2}$	Easy to evaporate. Large loss.

Table 1  
Mechanical loss of different kinds of thin metal film.

### Figure captions

#### Fig.1

Photo of the setup to pull fiber from silica rod; A silica rod is supported vertically from the rotating chuck. An oxygen-hydrogen flame from the movable torch melts the center of the rod. When the melted fiber's end passes in front of the refractive sensor, the flame is rotated away from the fiber to stop the melting.

#### Fig.2

Photo of the setup to coat fiber; The vacuum tank has two evaporation boats. The fiber is held vertically inside the cylindrical coating mask, which is designed to leave a uniform coating along the fiber. Both the mask and fiber are rotated during evaporation. Thickness monitor was put outside of the mask. A glass plate is shown outside of the mask, which was used to record the thickness and uniformity of the coating so that the mask shape could be determined.

#### Fig.3

Effect of the coating mask; Vertical and horizontal axes represents coating thickness and vertical location from the bottom end of suspended fiber, respectively. The thickness variations were measured by monitoring the transmission of laser light through coatings on glass plates held both outside and inside the mask. Coating non-uniformity was corrected inside the mask down to  $\pm 10\%$  level.

#### Fig.4

Conceptual setup for the mechanical loss measurement using torsion pendulum; A pendulum is attached on the silica fiber end through a small cup. The rotational motion of the pendulum is detected by a shadow sensor, composed of an infrared LED and a silicon photodiode with an active area of  $10\text{mm} \times 10\text{mm}$ . The LED is driven by a stable voltage reference. The signal from the photodiode is amplified, filtered, and then logged by a PC. The PC has an software lock-in amplifier.

**Fig.5**

Dependence of measured fiber mechanical loss on fiber diameter; Square and round markers represent uncoated and coated fibers, respectively. The dotted line is the fitted model for the uncoated fiber data represented by Eq.(2). The coating material used here is Bi (to provide conductivity) and Ge (which was used as an adhesive under layer). (A) and (B) correspond to the data shown in Fig. 6.

**Fig.6**

Examples of decay curve; (A): uncoated fiber with  $109\mu\text{m}$  diameter. (B): coated fiber with  $22\mu\text{m}$  diameter. Vertical and horizontal axes show oscillation amplitude in arbitrary unit and time in hour, respectively. Dashed lines are the fitted results.

**Fig.7**

Resistivity of coatings as a function of Bi and Ge thicknesses; Vertical and horizontal axes represent resistivity of Bi (in  $\Omega\text{m}$ ) and thickness of Bi coating (in  $\text{\AA}$ ). Round, square, and triangle markers represent 0 $\text{\AA}$ -, 50 $\text{\AA}$ -, and 100 $\text{\AA}$ -Ge under layer, respectively. Markers connected with lines represent the result with glass slides. The resistivity rapidly increases with decreasing Bi thickness, with an onset determined by the Ge thickness. Horizontally flat part was regarded as the region with continuous coating. Markers without the connecting lines represent the results with fibers.

**Fig.8**

Scanning electron microscope image of coated fiber; (a): Bi only coating. The thickness of Bi was 50 $\text{\AA}$ . Bright and dark parts are believed to represent variations in the growth directions of the Bi film. The spotted structure indicates the coating is not uniform, forming small crystal grains growing towards unorganized directions. (b): 300 $\text{\AA}$ -Bi coating (no sublayer) shows large scale grain structure. (c): 100 $\text{\AA}$ -Bi coating with 50 $\text{\AA}$ -Ge sublayer shows a more uniform film, indicating the adhesive effect of the Ge.

**Fig.9**

Sensitivity gain factor of conductive silica fiber compared to the best tungsten fiber; The vertical axis shows the gain obtained by the use of silica fiber in terms of spectrum force noise density, if compared with a tungsten fiber of loss  $\phi_{\text{fiber}} = 1/9000$  and diameter  $d = 20(\mu\text{m})$ . Horizontal axis represents silica fiber diameter  $d$  in  $\mu\text{m}$ . Thinner fibers have higher gain factors because they have a lower restoring force.

**Fig.10**

Force noise levels with tungsten and silica fibers together with LISA requirement; Vertical and horizontal axes show force noise spectrum density and frequency  $f$ . Dotted curve shows the noise level of the pendulum with tung-

sten fiber used in Ref.[4]; fiber diameter was  $25\mu\text{m}$  and  $\phi_{\text{fiber}} = 1/1700$  in this experiment. Thick solid curve shows the noise level with silica fiber. We used same parameters except for the diameter ( $22\mu\text{m}$ ), loss ( $\phi_{\text{fiber}} = 1/(9.5 \times 10^4)$ ), and shear modulus. These conductive silica fiber values were demonstrated in this investigation. We assumed identical readout sensor noise for these two curves. The sensor noise corresponds to the  $f^2$  rise at higher frequency. The  $f^{-1/2}$  line at lower frequency is the thermal noise-limited part. The curve on the bottom is the LISA GRS requirement [3].

**Fig.11**

Comparison of measured averaged coating loss and expected (modeled) loss; Vertical axis shows the measured averaged loss, which was calculated from measured fiber loss  $\phi_{\text{fiber}}$ , modeled silica loss  $\phi_{\text{SiO}_2}$  (Eq.(2)), and Eq.(4). Horizontal axis represents the expected averaged loss  $\phi_{\text{avg}}$  calculated independently from Table 1 and Eq.(2). The top middle marker is the data from the thinnest ( $11\mu\text{m}$ ) coated fiber.



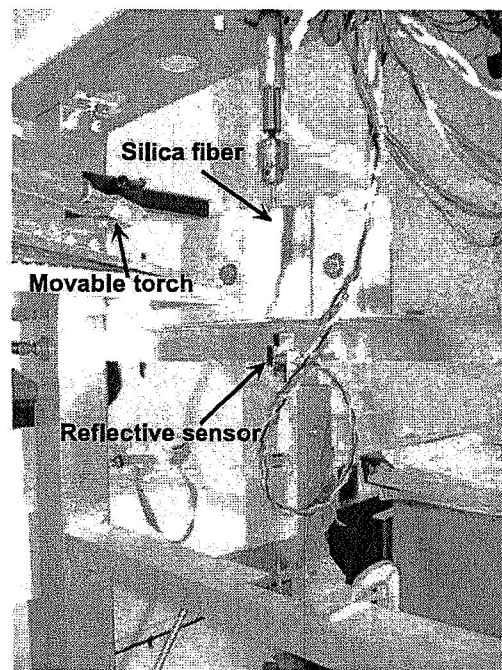


Fig. 1.

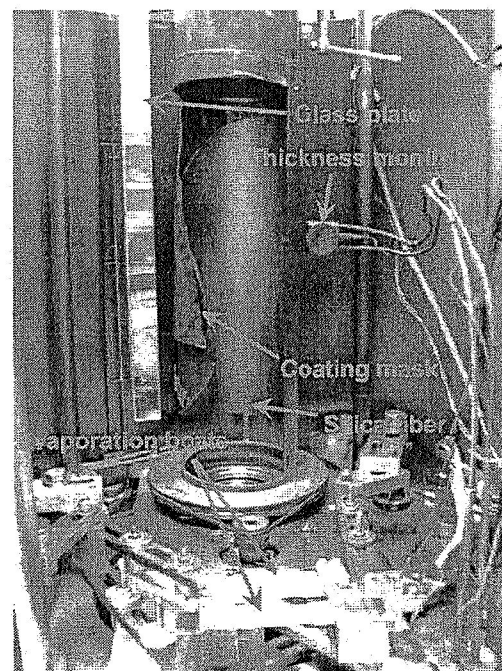


Fig. 2.

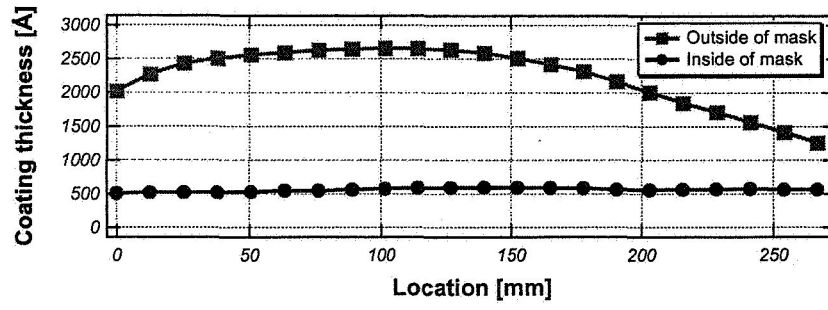


Fig. 3.

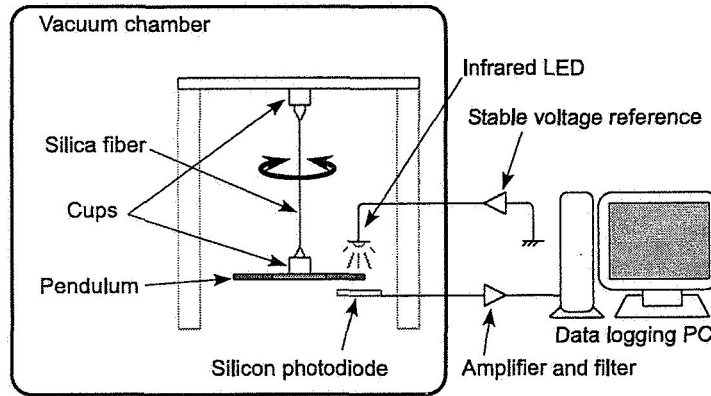


Fig. 4.

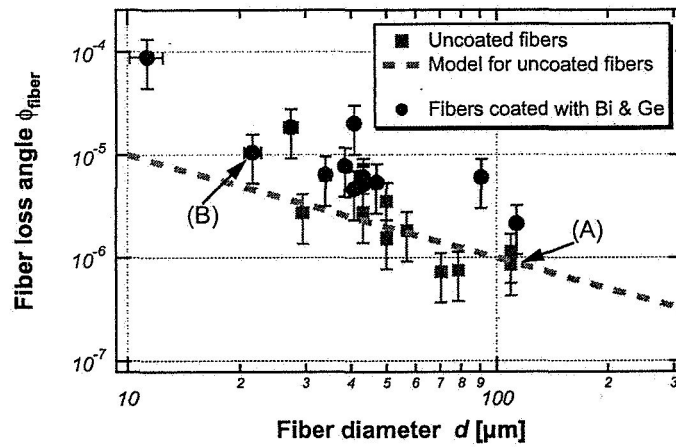


Fig. 5.

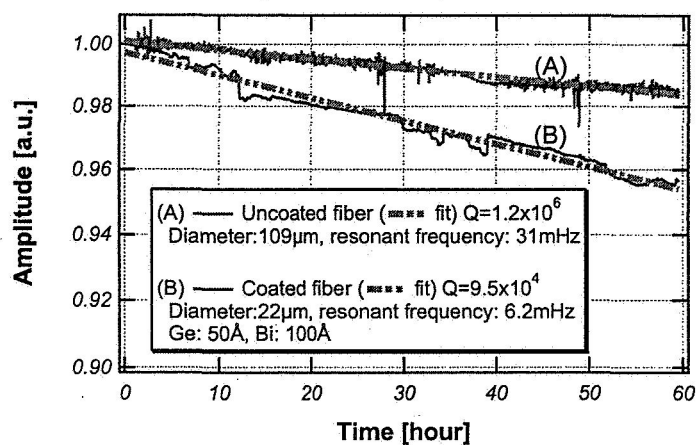


Fig. 6.

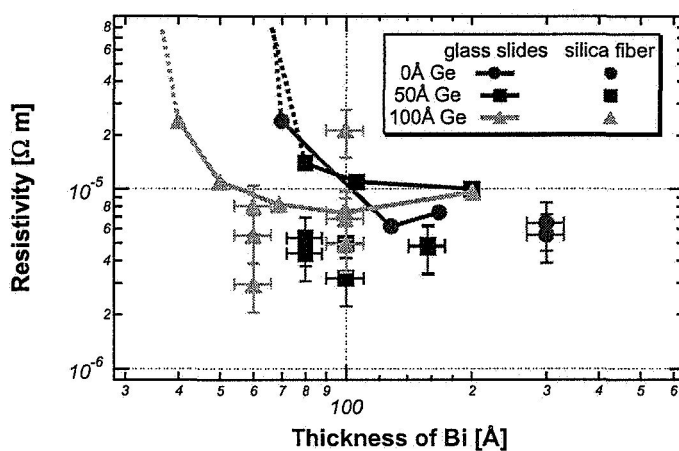


Fig. 7.

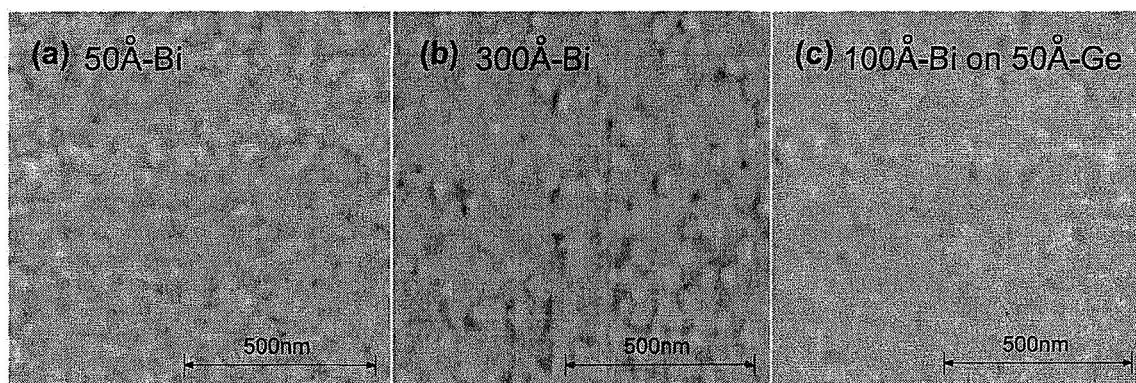


Fig. 8.

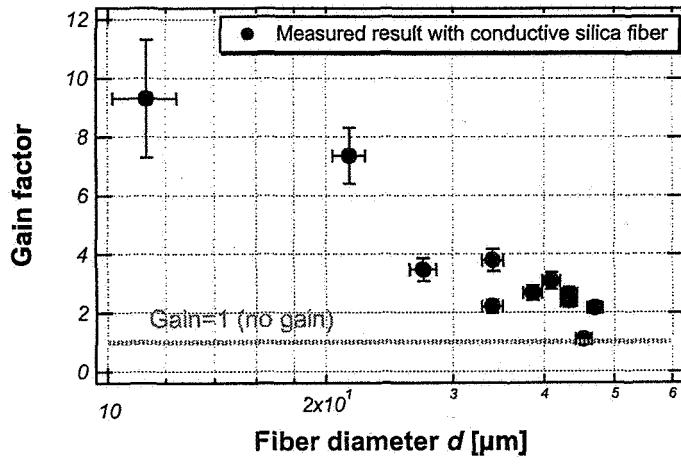


Fig. 9.

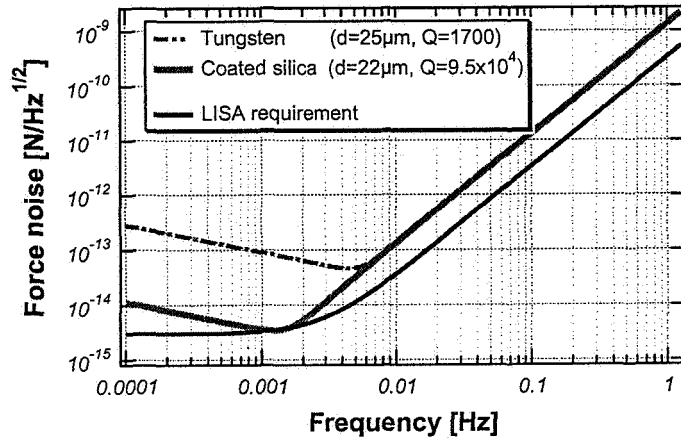


Fig. 10.

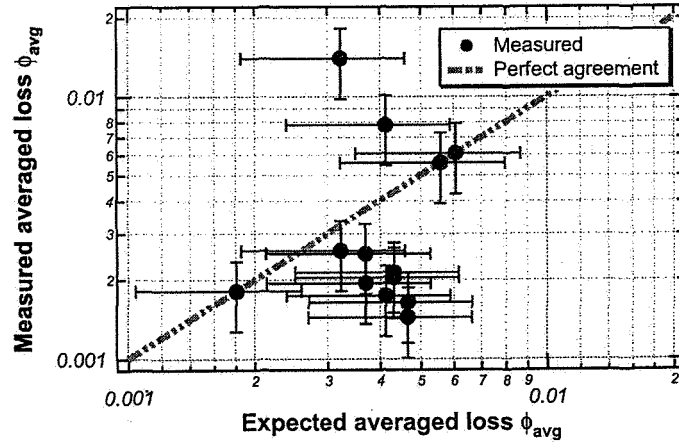


Fig. 11.